ICAS 2020 SHANGHAI
International Council of the Aeronautical Sciences
32nd Congress of the International Council of the Aeronautical Sciences
September 6-10, 2021
Pudong Shangri-La, Shanghai, China

INFLUENCE OF AERODYNAMIC ASYMMETRY ON SPIN PARAMETERS OF THE COMMON RESEARCH MODEL

Alexander N. Khrabrov[1], Maria E. Sidoryuk[1]

[1]Central Aerohydrodynamic Institute (TsAGI), Zhukovsky, Russia

Abstract

Aerodynamic asymmetry plays an important role in spin behavior of fighters, making some of spins unrecoverable. In this work, the influence of the varying value of the lateral aerodynamic asymmetry on the spin parameters of a transport aircraft is studied by direct calculation of spin parameters applying continuation on a parameter technique. The sensitivity of spin modes to uncertainties in other aerodynamic parameters is studied using robust analysis tools (μ-analysis).

Keywords: aerodynamic asymmetry, uncertainty, aircraft spin, robust analysis

1. Introduction

Reliable prediction of aircraft spin and other critical regimes is entirely related to the adequacy of the aerodynamic model used for the analysis. It is known that aerodynamic asymmetry plays an important role in stall and spin behavior of fighters. Due to the yaw asymmetry, the right spins can significantly differ from the left ones, and flat spin modes can become unrecoverable [1]. The aim of this work is to investigate the influence of aerodynamic asymmetry on the parameters of the spin modes of a transport aircraft. In this study, NASA Common Research Model (CRM), a long-haul aircraft is used. CRM was developed by NASA and Boeing for comparative experimental and numerical studies. The model geometry, including the 3D mathematical model of the surface, is taken from [2]. For NASA CRM, a series of experimental studies of stationary aerodynamics at high speeds, including transonic ones, were carried out in various wind tunnels in the USA, Europe and Japan, and a number of investigations of dynamics were carried out [3].

TsAGI has produced a dynamically scaled NASA CRM model. It was designed for different aerodynamic and dynamic studies. The mathematical model of aerodynamics is built on the basis of measurements of aerodynamic efforts in two low-speed TsAGI wind tunnels during static, forced oscillatory, and rotary balance tests in a wide range of angles of attack, sideslip angles, angular rates and various controls deflections, from ordinary flight to the post-stall region. Comparison of similar aerodynamic characteristics obtained in two different wind tunnels demonstrates a random sign of aerodynamic asymmetry that occurs at zero sideslip and zero angular rate in some ranges of angle of attack due to flow separation. The value of this asymmetry, as all measured parameters, has an uncertainty, especially since all spin-tunnel models operate at very low Reynolds numbers compared to full-scale aircraft. A significant influence of the uncertainties of some aerodynamic characteristics on the spin parameters was found in [4] for a light aircraft. The value of the aerodynamic asymmetry depends on the features of the flow separation, and in this work it is assumed that it varies from zero to the maximum values observed in wind tunnel experiments. The possible influence of uncertainties in other aerodynamic parameters is also taken into account.

The influence of aerodynamic asymmetry is studied by direct calculation of the spin parameters for various values of the asymmetry of the lateral characteristics of the developed aerodynamic model using continuation on a parameter technique [5-7] and related methods of bifurcation and stability analysis. The influence of uncertainties in other aerodynamic parameters on the obtained spin parameters is studied using robust analysis tools (μ-analysis) [8].

2. Aerodynamic Model

2.1 Scaled CRM model

A general view of the CRM model in the TsAGI low speed wind tunnel is shown in Fig.1. The scaled CRM model has the following parameters: wing span b=1.2 m, wing mean chord $\bar{c} = 0.143\,m$, reference wing area S=0.16m^2, inertia matrix I = diag (I_x, I_y, I_z) = diag (0.110, 0.245, 0.389) kg·m^2. The original CRM has no control surfaces. The TsAGI model was supplemented with a common set of control surfaces driven by servos: elevator, ailerons and rudder.

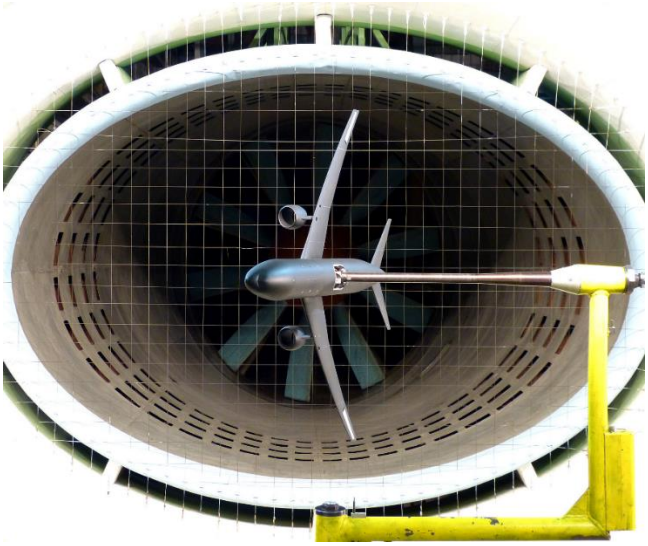

Figure 1 – CRM model in the TsAGI wind tunnel.

2.2 Aerodynamic model structure and main aerodynamic characteristics

An aerodynamic model for high angles of attack conditions is usually formulated by using experimental data obtained in a wind tunnel from static, small amplitude forced oscillations (in pitch, roll and yaw) and rotary balance tests. At high angles of attack, the aircraft motion with intensive rotation can strongly affect the separated flow, and the aerodynamic coefficients become highly dependent on the aircraft conical rate. This dependence can be described as follows [1,4]:

$$C_i = C_{i_{s.r.}}(\alpha, \beta, p_a, \delta) + C_{iq_a} q_a + C_{ir_a} r_a$$

where C_i ($i = X, Y, Z, l, m, n$) are the coefficients of dimensionless aerodynamic forces and moments, α and β are the angles of attack and sideslip, $\delta = (\delta_e, \delta_a, \delta_r)$ are the deflections of elevator, aileron and rudder, p_a, q_a and r_a are roll, pitch and yaw rate projections of angular rate on wind axes respectively, related to the body axes angular rates p, q, r as follows:

$$\begin{aligned} p_a &= p\cos\alpha\cos\beta + r\sin\alpha\cos\beta + q\sin\beta \\ q_a &= -p\cos\alpha\sin\beta - r\sin\alpha\sin\beta + q\cos\beta \\ r_a &= p\sin\alpha - r\cos\alpha \end{aligned}$$

where p_a coincides with the rate of rotation in rotary balance tests, and r_a, q_a, components represent misalignment between velocity and angular velocity vectors. The misalignment components are usually small with respect to rotary balance rate. The force and moment coefficients representation used in the work for spin parameter calculation is the following:

$$
\begin{aligned}
C_X &= C_X(\alpha,\beta)+C_X(\alpha,p_a)+\Delta C_X(\alpha,\delta_e)\\
C_Z &= C_Z(\alpha,\beta)+C_Z(\alpha,p_a)+\Delta C_Z(\alpha,\delta_e)\\
C_Y &= C_{Y0}(\alpha)+\Delta C_Y(\alpha,\beta)+\Delta C_Y(\alpha,p_a)+\Delta C_Y(\alpha,\delta_a)+\Delta C_Y(\alpha,\delta_r)\\
C_m &= C_m(\alpha,\beta)+\Delta C_m(\alpha,p_a)+\Delta C_m(\alpha,\delta_e)+C_{mq_a}q_a\\
C_l &= C_{l0}(\alpha)+\Delta C_l(\alpha,\beta)+\Delta C_l(\alpha,p_a)+\Delta C_l(\alpha,\delta_a)+\Delta C_l(\alpha,\delta_r)+C_{lq_a}q_a+C_{lr_a}r_a\\
C_n &= C_{n0}(\alpha)+\Delta C_n(\alpha,\beta)+\Delta C_n(\alpha,p_a)+\Delta C_n(\alpha,\delta_a)+\Delta C_n(\alpha,\delta_r)+C_{nq_a}q_a+C_{lr_a}r_a
\end{aligned}
\qquad (1)
$$

The lateral coefficients $C_i\ (i=Y,l,n)$ in formula (1) contain separate terms $C_{i0}(\alpha)$ to emphasize the significance of the lateral asymmetry that is caused by the asymmetric flow separation in the stall region. Figure 2 shows the results for $C_{l0}(\alpha)$, $C_{n0}(\alpha)$, and $C_{Y0}(\alpha)$, obtained with zero sideslip in the TsAGI wind tunnels T-103 and T-105. Three areas of asymmetry are observed in the T-103: $\alpha=10^\circ\div14^\circ$ - asymmetric flow separation on the wing, $\alpha=24^\circ\div28^\circ$ - asymmetric flow separation around the engine nacelles and the most noticeable asymmetry at $\alpha=50^\circ\div70^\circ$, apparently related to the asymmetry of the separated flow around fuselage nose. It should be noted that the last observed asymmetry has different signs when measured in T-103 and T-105 wind tunnels. In addition, the asymmetry at $\alpha=10^\circ\div14^\circ$ is not observed in the T-105 wind tunnel. For this reason, the regions of asymmetry at $\alpha=24^\circ\div28^\circ$ and $\alpha=50^\circ\div70^\circ$ were taken into account in the mathematical model, and the functions of its description are included in the model with a multiplicative parameter that makes it possible to scale or nullify the contribution of the asymmetry or change the sign of its influence.

To facilitate the implementation of the continuation technique, the nonlinear experimental dependencies $\Delta C_i(\alpha,\beta)$ $(i=Y,l,m,n)$ in (1) are approximated by 3-rd order polynomials of β. The nonlinear functions $\Delta C_i(\alpha,p_a)$ $(i=Y,l,n)$ are similarly approximated by 3-rd order polynomials of p_a using the standard least-square approach. The dependence of the roll and yaw moment coefficients of the CRM model on angle of attack and sideslip is presented in Fig. 3, and the dependence of roll and yaw moment coefficients on angle of attack and non-dimensional angular rate $\omega=p_ab/(2V)$ (V is the magnitude of the aircraft velocity) is presented in Fig. 4.

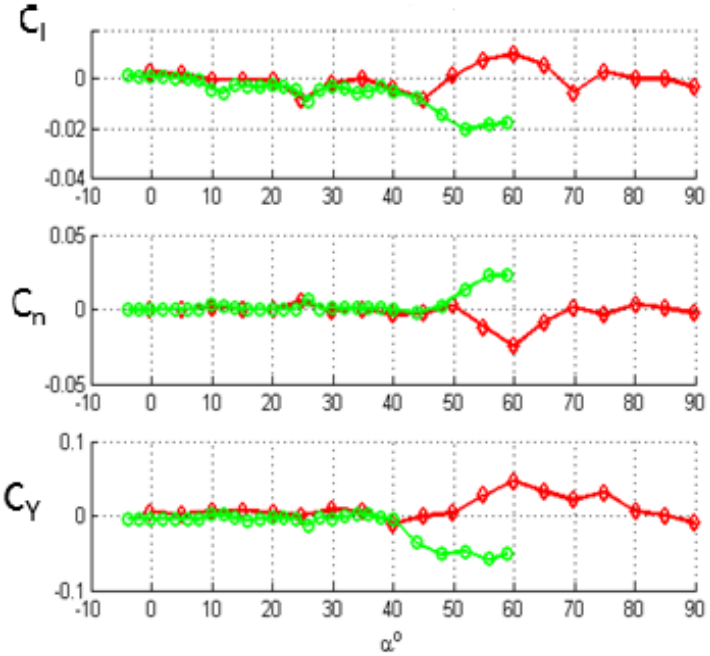

Figure 2 – Dependence of lateral static coefficients on angle of attack at zero sideslip obtained in two different wind tunnels.

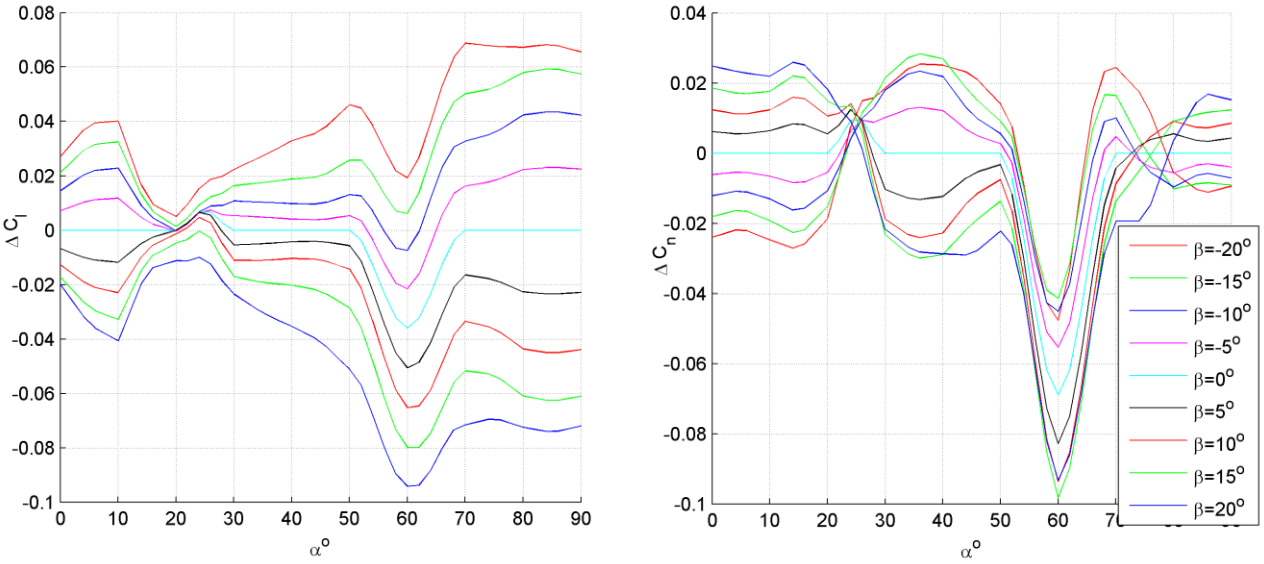

Figure 3 – Dependence of roll and yaw moment coefficients on angle of attack and sideslip.

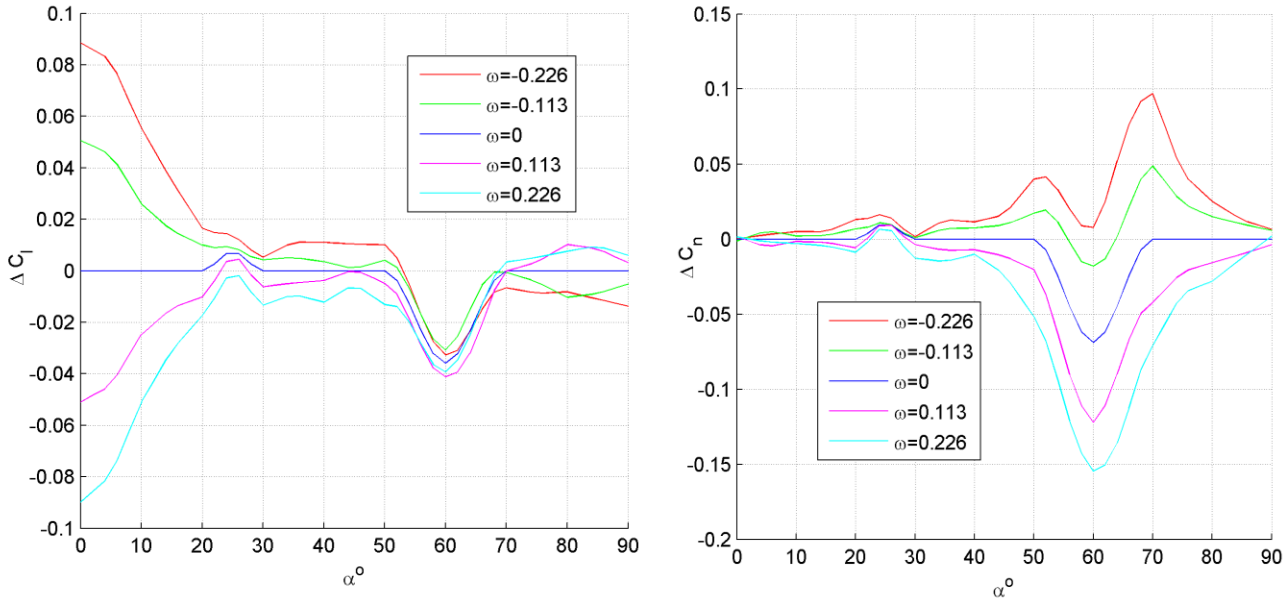

Figure 4 – Dependence of roll and yaw moment coefficients on angle of attack and non-dimensional conical angular rate.

3. Calculation of spin parameters

The calculation of spin and other critical regimes and its dependence on aerodynamic asymmetry is carried out using the standard technique of numerical continuation of equilibrium and periodic solutions of nonlinear aircraft dynamics on a parameter [5-7]. The usual way to analyze the aircraft spin dynamics is to consider the 8-th order autonomous system of motion equations obtained from the complete six-degree of freedom motion equations under the assumption of a fixed altitude using the aerodynamic model (1):

$$\dot{x} = F(x, \delta) \tag{2}$$

where the state vector is $x = (V, \alpha, \beta, \theta, \phi, p, q, r)' \in R^8$, and the control vector is $\delta = (\delta_e, \delta_a, \delta_r)'$. The yaw angle $\dot{\psi} = (r\cos\phi + q\sin\phi)/\cos\theta$ which indicates the aircraft rotation, is determined by

independent integration. In the procedure of continuation, the deflection of one of the control surfaces is used as a parameter, and two others are fixed. The thrust is considered equal to zero. The equilibrium states are determined by the system of algebraic equations:

$$F(x,\delta)=0 \tag{3}$$

The starting points of curves (3) in R^9 can be found by approximate methods [1]. When calculating equilibria their local stability is also analyzed using a linearized system of equations. The continuation of limit cycles or periodic solutions is performed by solving the parameter dependent boundary-value problem:

$$x(T,\delta)-x(0,\delta)=0$$

3.1 Sensitivity of spin parameters to lateral aerodynamic asymmetry

Figures 5 and 6 show examples of the equilibrium parameters and amplitudes of limit cycle solutions depending on the aileron deflection at δ_e = -15°, δ_r = 0, for the value of asymmetry parameter coinciding with that observed in T-103, and for the symmetrized model of aerodynamics, respectively. Different colors correspond to different stability properties (qualitatively different distributions of the equilibrium eigenvalues), see Fig.7. Stable solutions that occur in flight are shown in red. For periodic solutions, only stable ones are shown. The spin modes observable in flight correspond to stable equilibrium solutions (steady spin) or stable periodic solutions (oscillatory spin). It can be seen that the differences between the bifurcation diagrams in Fig. 5 and 6 lies mainly in the range of angles of attack $\alpha = 24° \div 35°$.

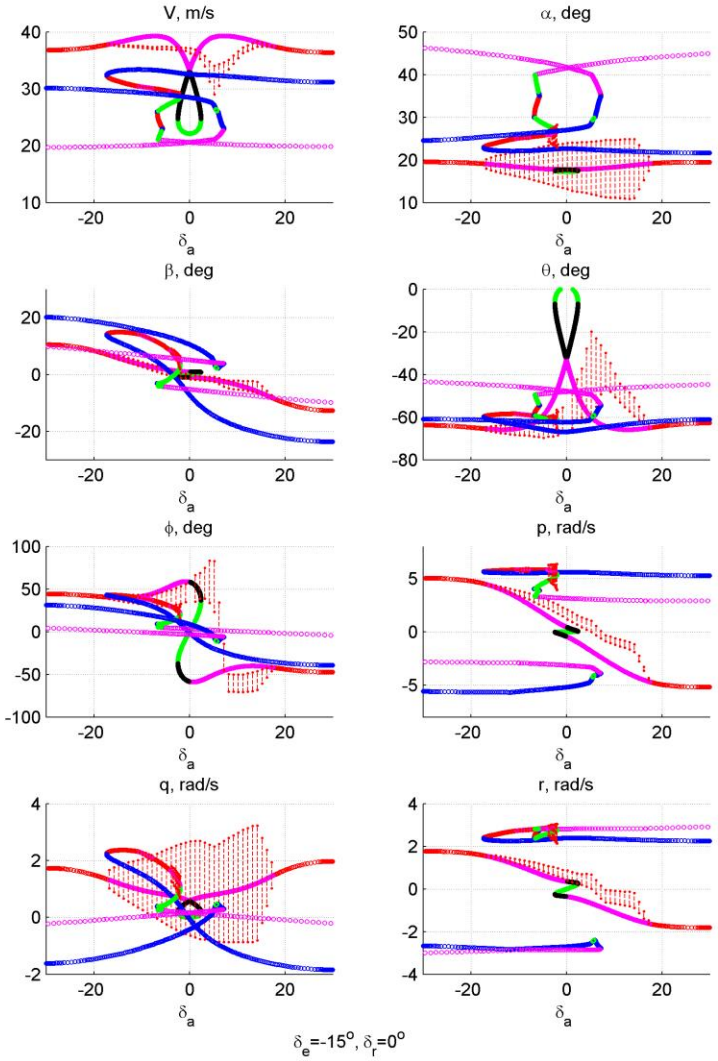

Figure 5 – Steady-states and limit cycle solutions depending on the aileron deflection, δ_e = -15°, δ_r = 0, with asymmetry.

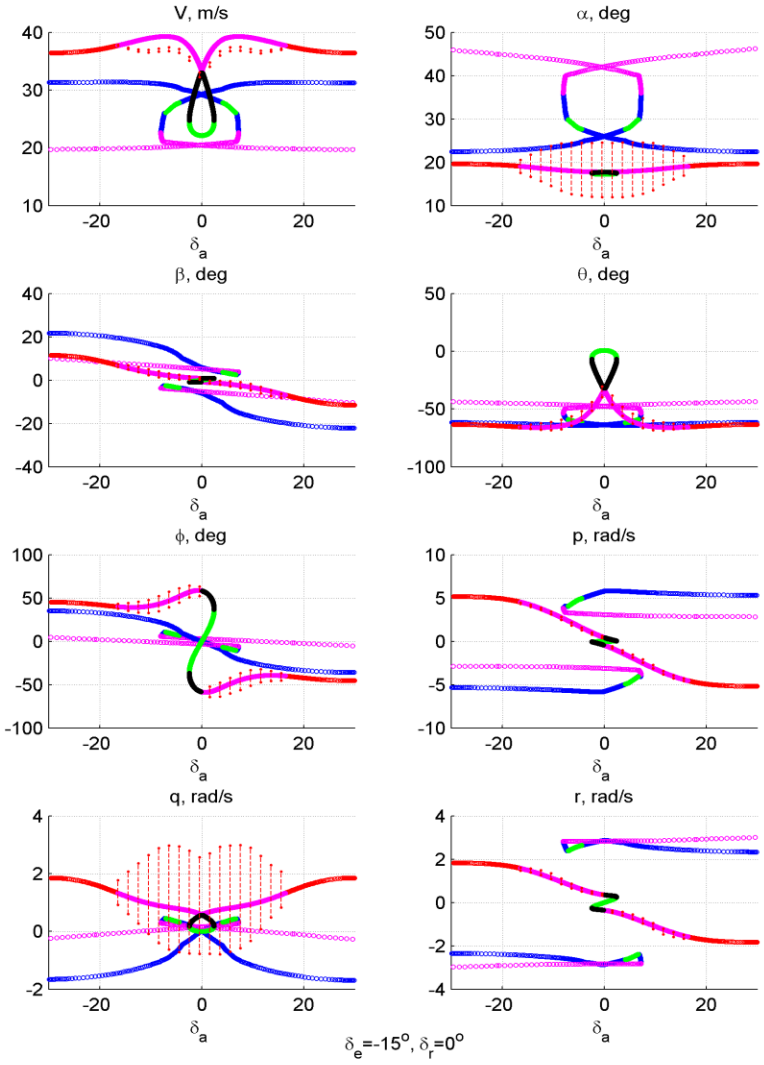

Figure 6 – Steady-state and limit cycle solutions depending on the aileron deflection, δ_e = -15°, δ_r = 0, symmetric case.

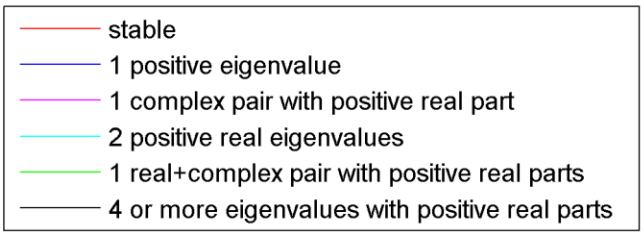

Figure 7 – Color codes for qualitatively different distributions of equilibrium eigenvalues.

In the case of asymmetry, there are ranges of very steep spins at $\delta_a = -17° \div 0°, \alpha = 23° \div 25°$, and $\delta_a = -4° \div 0°, \alpha = 30° \div 25°$, which are absent in the symmetric case. The first range of these spin solutions (steady or oscillatory) is caused solely by aerodynamic asymmetry, the second range is caused by other aerodynamic uncertainties. It can appear or disappear with a slight change of the symmetrical aerodynamics, as shown in Fig. 8. The trajectories of stable oscillatory spins caused by aerodynamic asymmetry are shown in Fig. 9 for several aileron deflections.

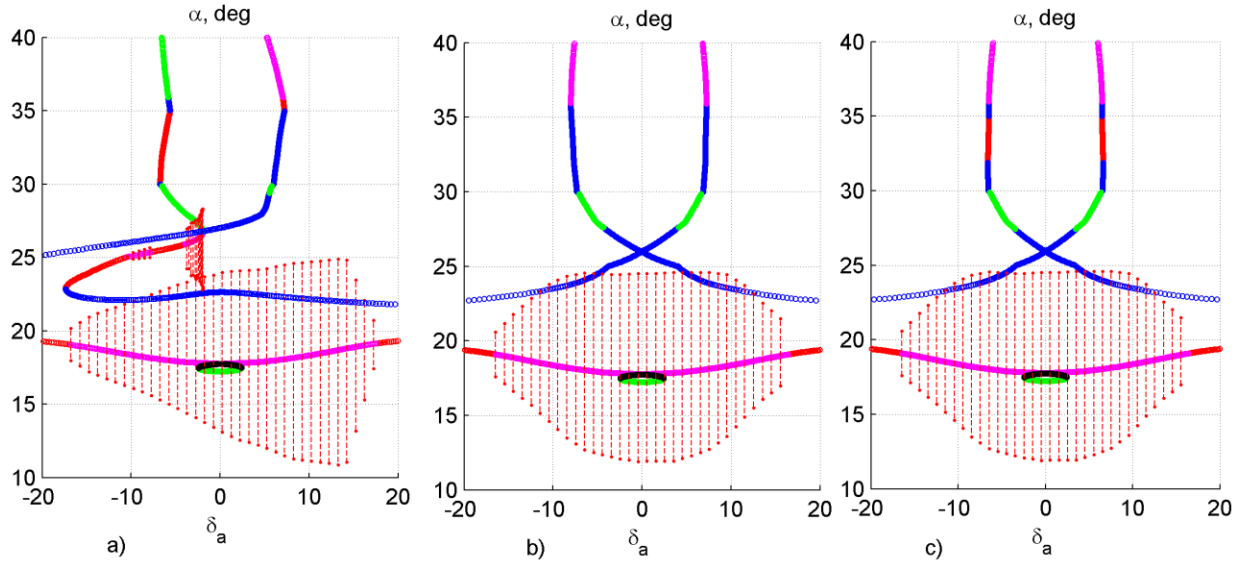

Figure 8 – Comparison of steady-state and limit cycle solutions depending on the aileron deflection, $\delta_e = -15^o$, $\delta_r = 0$, a) with asymmetry, b) without asymmetry, c) without asymmetry, with uncertainties.

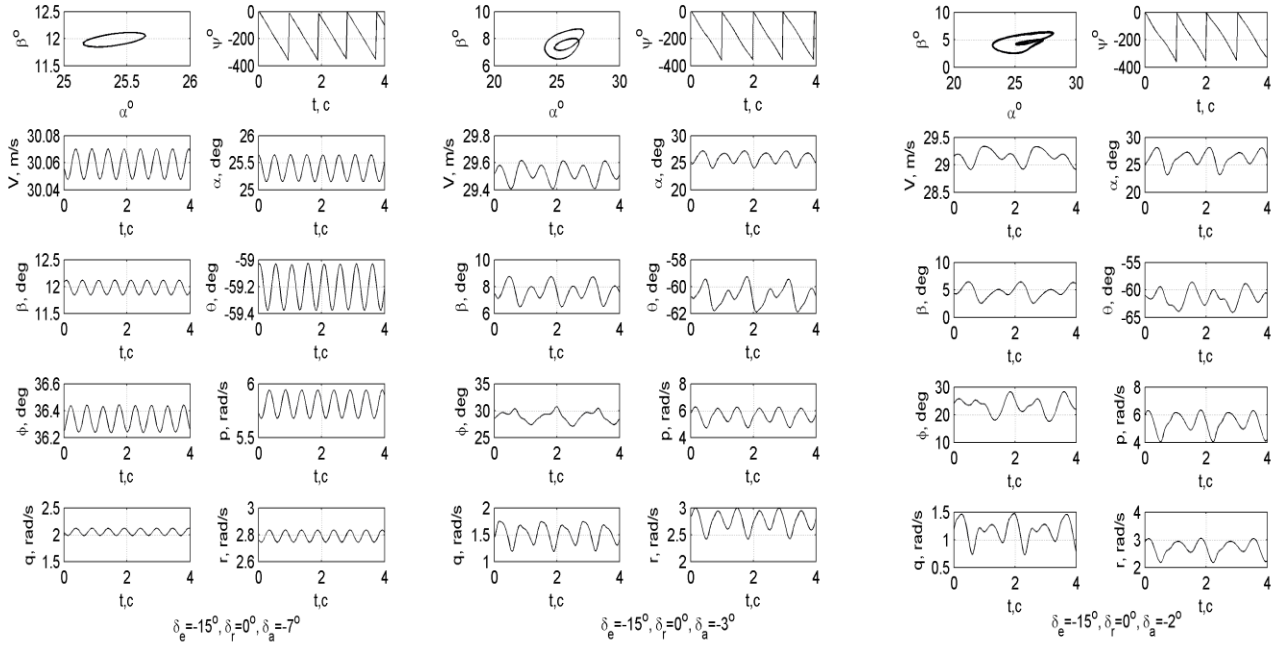

Figure 9 –Trajectories of stable oscillatory spins caused by aerodynamic asymmetry, depending on the aileron deflection.

Since the aerodynamic asymmetry is a very uncertain parameter, it is therefore necessary to analyze the spin dependence on its value. Figures 10 and 11 show steady-state spins for different values of aerodynamic asymmetry (only three components from the eighth-length state vector are here presented: *α, β, p*). It can be seen that the range of spins decreases considerably with decreasing aerodynamic asymmetry, and for a level of asymmetry equal to 25% of its nominal value, there is no spin. Thus, to reliably predict the aircraft spin in flight, it is important to have an accurate estimate of the magnitude of the aerodynamic asymmetry and accurately transfer it from the wind tunnel conditions for a scaled model to the actual flight of the aircraft.

Note that other stable equilibria and limit circles in Figs. 5-6 at $\alpha \sim 20^o$ are practically independent of the aerodynamic asymmetry. They describe self-induced oscillations that transform into autorotation

motion with increasing aileron deflection.

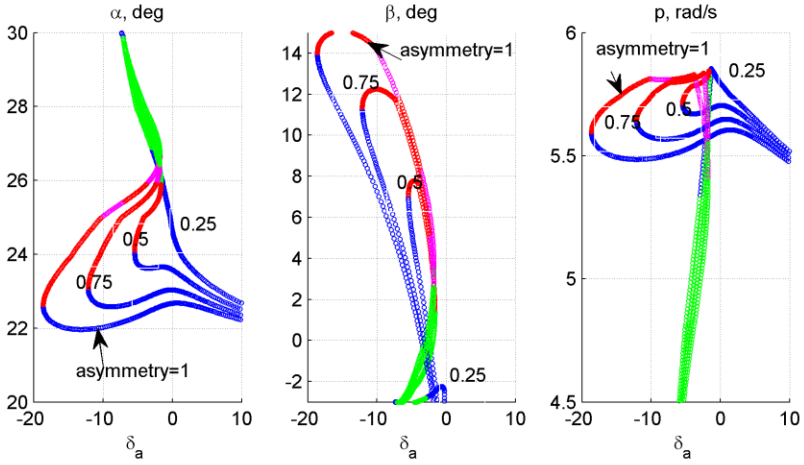

Figure 10 – Steady-state spins at different values of aerodynamic asymmetry, ω>0.

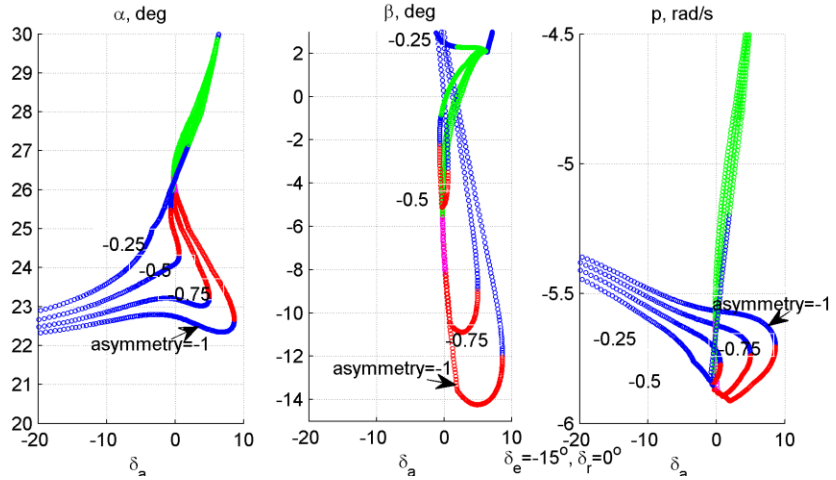

Figure 11– Steady-state spins at different values of aerodynamic asymmetry, ω<0.

Another significant range of aerodynamic asymmetry is at angles of attack $\alpha = 50° \div 70°$. To find the possible spin regimes at these high angles of attack, the equilibrium solutions were calculated similarly, continuing on deflections of different control surfaces. Figures 12 and 13a) show such examples at a high level of aerodynamic asymmetry. It can be seen that there are no stable solutions that could cause spin in flight. The analysis shows that in the entire permissible range of control surfaces deflections, there are also no limit circles (corresponding to oscillatory spins). With zero aerodynamic asymmetry, there are no equilibrium solutions at high angles of attack. Thus, at high angles of attack for the considered mathematical model of the CRM aerodynamics, there are no spin modes affected by aerodynamic asymmetry.

To make sure of this, the aerodynamic model with uncertainties was also considered, since uncertainties can sometimes lead to a significant change in the spin picture [4]. For the worst-case roll and yaw moment uncertainties (largest range of equilibrium solutions), the equilibria caused by aerodynamic asymmetry versus elevator deflection are shown in Fig.13b) for uncertainty levels of 10 and 15%. It can be seen that in this case there are also no stable solutions (spin modes).

Steady-state steep spins at moderate α caused by aerodynamic asymmetry, depending on the elevator deflection, and different δ_a or δ_r are shown in Figs.14 and 15, respectively. It can be seen that in this case, the region of spins is noticeable.

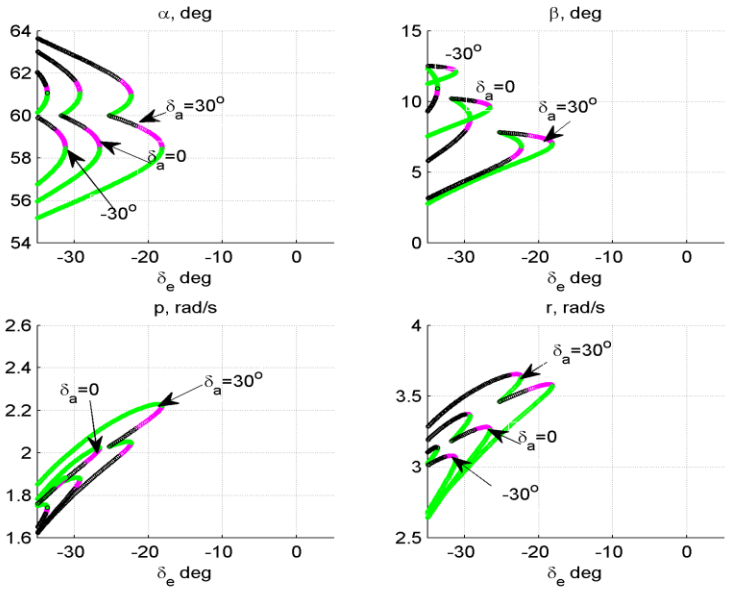

Figure 12 – Equilibrium solutions at high angles of attack due to the aerodynamic asymmetry depending on the elevator deflection.

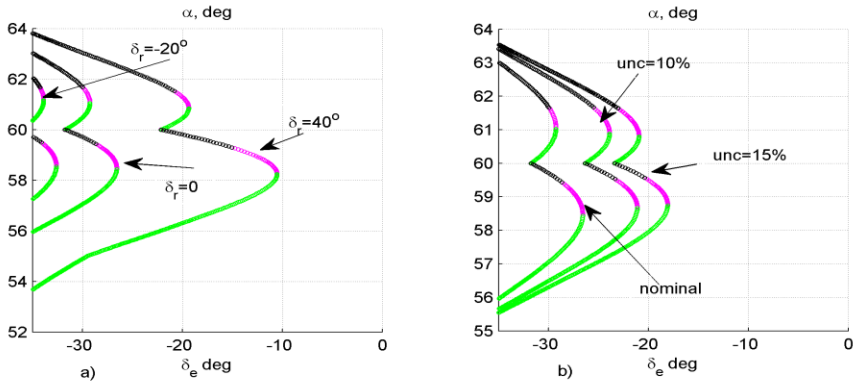

Figure 13– Equilibria at high angles of attack due to aerodynamic asymmetry depending on the elevator deflection a) at different rudder deflections b) uncertainties of static yaw and roll moments.

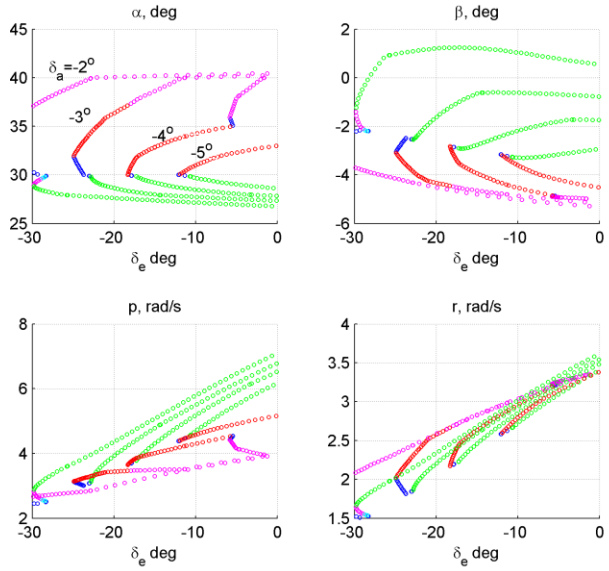

Figure 14 – Equilibria and steady-state spins (red) due to aerodynamic asymmetry depending on the elevator deflection and varied δ_a.

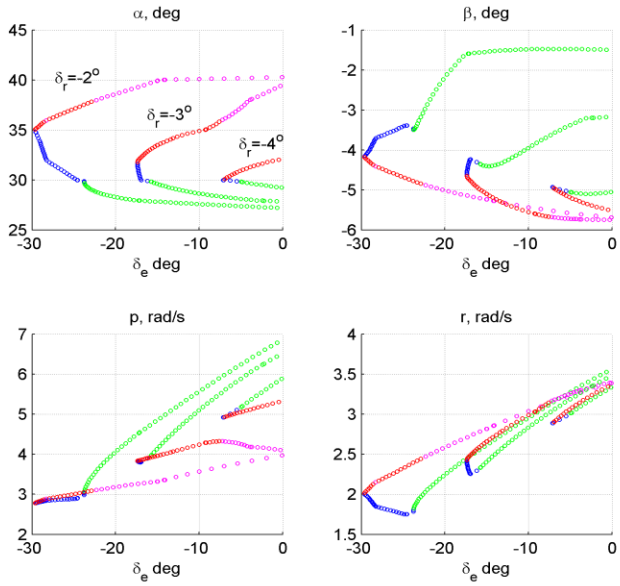

Figure 15 – Equilibria and steady-state spins due to aerodynamic asymmetry depending on the elevator deflection, and varied δ_r.

4. Sensitivity of the parameters of spins caused by aerodynamic asymmetry, to uncertainties of other aerodynamic parameters

It was found in [4] that the uncertainties of the aerodynamic model can significantly affect the bifurcation diagrams calculated for predicting spin and spin parameters. The values of the uncertainties included in the aerodynamic model in [4] were determined from a series of repeated measurements of static characteristics of a light aircraft for various combinations of angle of attack and sideslip, different methods of model suspension, various flow rates in the wind tunnel. The analysis was performed by directly calculating the spin parameters using the continuation on a parameter technique.

In this work, we use another approach to analyzing the sensitivity of the spin parameters to the uncertainties of the aerodynamic model. Consider any stable spin equilibrium caused by aerodynamic asymmetry (Figs. 10, 11). Its stability is determined by calculating the eigenvalues of an 8-th order system linearized near this stable spin equilibrium x_S:

$$\Delta\dot{x} = A\Delta x,\ A = \left.\frac{\partial F}{\partial x}\right|_{x_S} \tag{5}$$

To determine whether the spin equilibrium x_S remains stable when aerodynamic parameters vary near their nominal values in model (1), it is possible with using the robust stability analysis [6], in particular, using the structured singular value (μ) analysis, which allows to estimate the robust stability and its margins for the interconnection

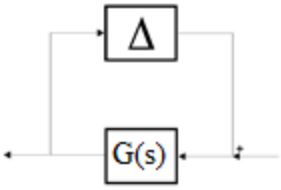

where *G(s)* is linear time invariant system described by equation (5) and $\Delta=\mathrm{diag}(\Delta_1, \ldots, \Delta_n)$ is, in our case ,a bounded time invariant uncertainty, $|\Delta_i| < \beta_i$. The μ – analysis guarantees robust stability, that is asymptotical stability of the uncertain system for all values of the modeled uncertainty within the given bounds, if μ (the upper bound of the structured singular value) is less than 1.

Since the considered model of aerodynamics is heuristic, all parameters are uncertain. It was found [4] that the uncertainties of the roll and yaw moment coefficients have an especially large effect on the spin parameters. For this reason, we consider here as uncertain derivatives $C_{l\alpha}$, $C_{l\beta}$, C_{lp}, C_{lr}, $C_{n\alpha}$,

$C_{n\beta}$, C_{np}, C_{nr}, all together or separately, calculated near several spin equilibrium x_S due to aerodynamic asymmetry. This means that elements (6,2), (6,3), (6,6), (6,8), (8,2), (8,3), (8,6), (8,8) of matrix A in Eq.(5) (remembering that the state vector is $\mathbf{x} = (V, \alpha, \beta, \theta, \phi, p, q, r)' \in R^8$), are uncertain.

Assume that the uncertainty value of each of these derivatives is 10%. Figure 16 shows the mu values calculated for the cases of one of the listed uncertainties or all of them together. It can be seen that the system can lose stability in the case of all uncertain derivatives for the first spin mode (α=23.06°), but remains robustly stable in all three other cases. Note that if the equilibrium becomes unstable, this does not mean that the spin disappears: the steady-state spin can become oscillatory (the answer can be given using bifurcation analysis).

The value $\text{margin} = 1/\mu$ gives the stability margin of an uncertain system: the system is stable if the norm of i-th uncertainty is less than $\text{margin} \times \beta_i$. Figure 16 allows to estimate the uncertainty of which derivative has greater effect on the robust stability of spin: in this case it is the derivatives C_{lp} and $C_{n\alpha}$.

In the case of robust stability analysis of spin equilibrium, the larger the stability margin, the more dangerous this spin mode. In other words, this spin mode exist despite an inaccurate knowledge of the aircraft aerodynamics. Thus, the robust stability test can provide some information about the danger of the spin regime, in addition to another danger metric: the size of its region of attraction [9].

Figure 17 shows changing of the bifurcation diagram (a part of Fig. 5) at different uncertainties of yaw and roll moments within the considered limits. It can be seen that steep spin at $\alpha = 30° \div 35°$ changes insignificantly, but the region of very steep spin at $\alpha = 23° \div 28°$ due to aerodynamic asymmetry can change considerably.

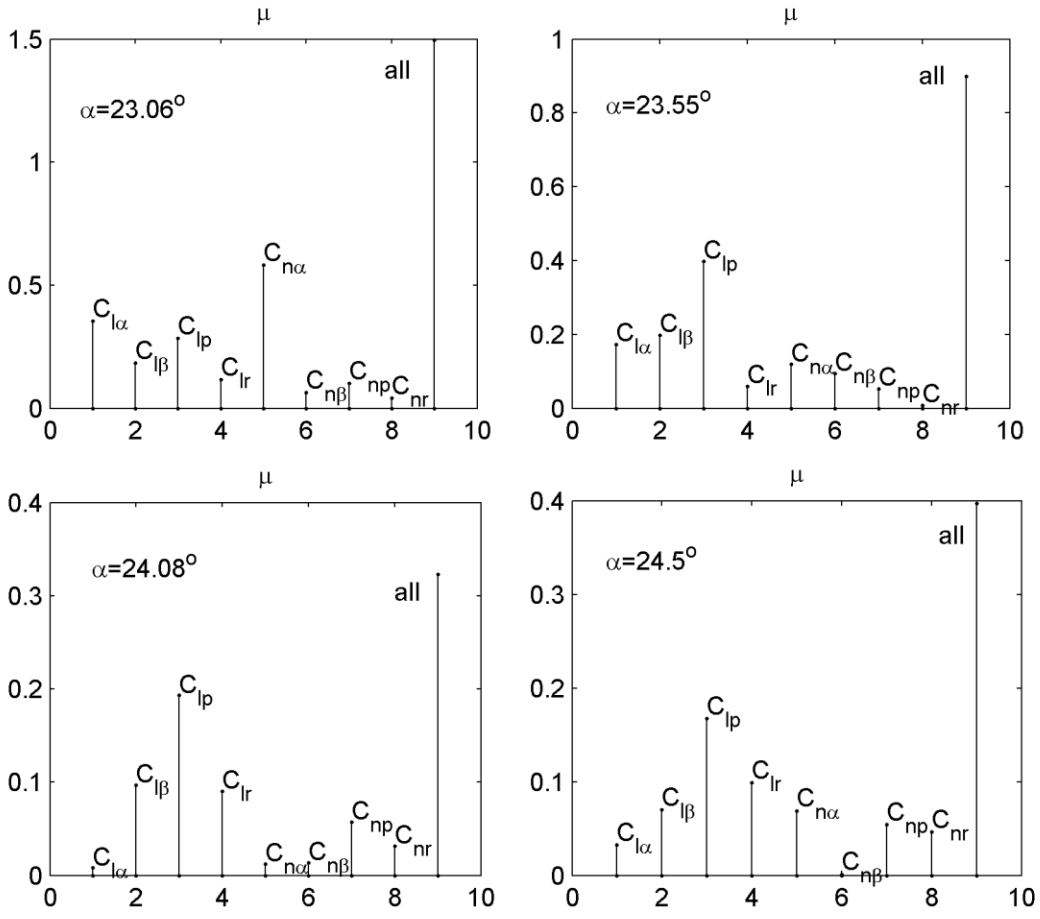

Figure 16 – Robust stability of spin regimes due to aerodynamic asymmetry at different aerodynamic uncertainties of yaw and roll moments.

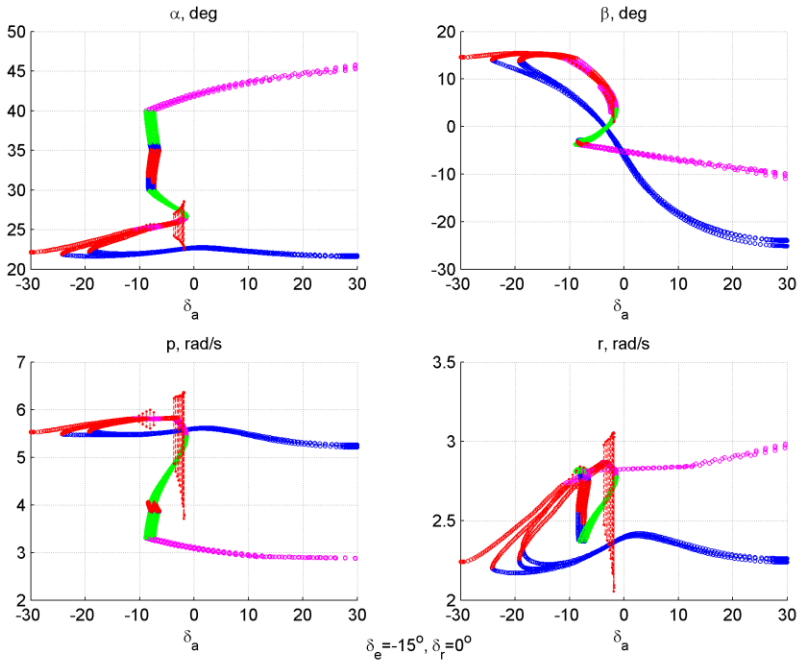

Figure 17 – Spins caused by aerodynamic asymmetry, depending on the aileron deflection, at different uncertainties of yaw and roll moments.

5. Spin recovery

Recovery from all the detected spin modes of CRM model, which occurred due to aerodynamic asymmetry, is possible by moving the controls to the neutral position. This recovery takes from 1 to 2 turns, see Fig.18. Improved methods allow to do this faster, but this is not the subject of this study.

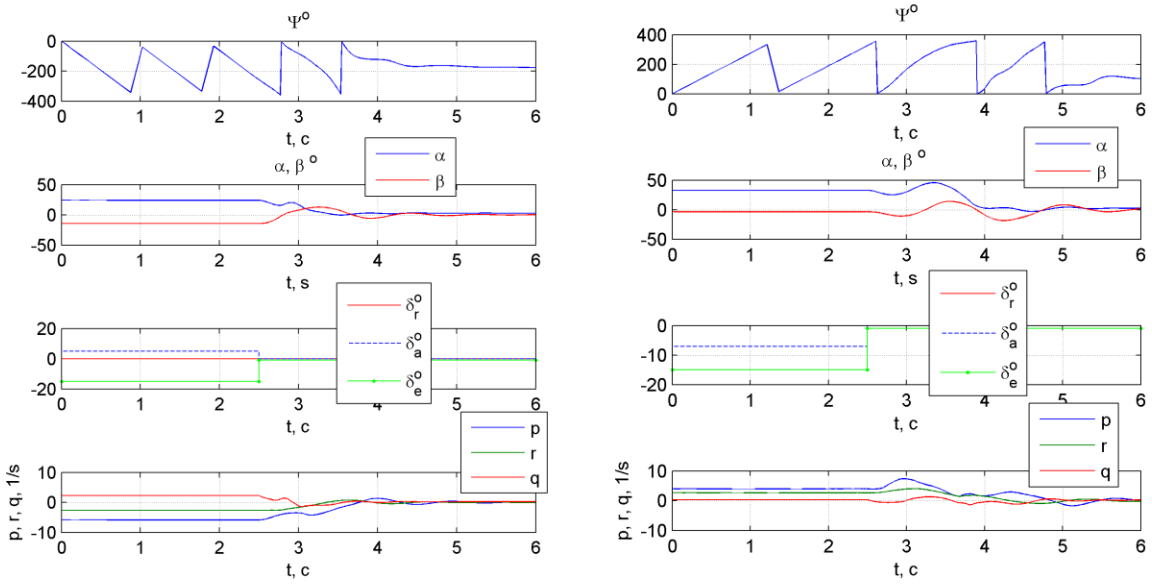

Figure 18 – Spin recovery by moving the controls to the neutral position.

6. Conclusions

The effect of lateral aerodynamic asymmetry on the spin parameters of the Common Research Model was studied using the direct calculation of the spin parameters applying the continuation on a parameter technique. It is established, that the range and the spin parameters can considerably

depend on the value of aerodynamic asymmetry, Thus, in order to reliably predict the aircraft spin in flight, it is important to be accurate in estimating the magnitude of the of aerodynamic asymmetry and translating it from wind tunnel conditions to actual flight of the aircraft. Robust stability analysis of spin equilibria allows to confirm the existence of spin in the presence of uncertainties in the aerodynamic coefficients, that is, despite inaccurate knowledge of the aerodynamics of the aircraft.

7. Contact Author Email Address

mailto: mariya.sidoryuk@tsagi.ru

8. Copyright Statement

References

[1] Goman, M. G., Khramtsovsky, A. V. Application of Continuation and Bifurcation Methods to the Design of Control Systems, *Philosophical Transactions of the Royal Society of London,* Series A—Mathematical, Physical, and Engineering Sciences, Vol. 356, No. 1745, pp 2277–2295, 1998. doi:10.1098/rsta.1998.0274.

[2] https://commonresearchmodel.larc.nasa.gov/geometry/ (accessed 25 May2021).

[3] Cen F., Li Q., Liu Z., Zhang L. and Jiang Y. Post-stall flight dynamics of commercial transport aircraft configuration: A nonlinear bifurcation analysis and validation. *J. Aerospace Engineering*, pp1-17, 2020.

[4] Farcy D., Khrabrov A., Sidoryuk M. Sensitivity of Spin Parameters to Uncertainties of the Aircraft Aerodynamic Model. *Journal of Aircraft*, Vol. 57, No. 5, 2020, pp. 1-16. doi: 10.2514/1.C035882

[5] Goman, M.G., Zagaynov, G.I., and Khramtsovsky, A.V. Application of Bifurcation Methods to Nonlinear Flight Dynamics Problems, *Progress in Aerospace Sciences*, Vol. 33, No. 59, 1997, pp. 539–586. doi:10.1016/S0376-0421(97)00001-8.

[6] Guicheteau P. Bifurcation theory: a tool for nonlinear flight dynamics, *Philosophical Transactions of the Royal Society of London*, Series A, 1998, No. 356, pp.2181-2201. Royal Society of London, Vol. 356, No. 1745, Oct. 1998, pp. 2297–2319.

[7] Lowenberg, M. H., Bifurcation Analysis of Multiple-Attractor Flight Dynamics, *Philosophical Transactions of the Royal Society of London*, Vol. 356, No. 1745, 1998, pp. 2297–2319. doi:10.1098/rsta.1998.0275

[8] Packard A., Balas G., Safonov M., Chiang R., Gahinet P., Nemirovski A., Apkarian P. *Robust control toolbox*, The Math Works Inc. Natick, 2016. http://www.mathworks.com/help/pdf_doc/robust/robust_ug.pdf.

[9] Sidoryuk M., Khrabrov A. Estimation of Regions of Attraction of Aircraft Spin Modes, *Journal of Aircraft*, Vol. 56, No. 1, 2019, pp. 205-216. doi: 10.2514/1.C034936.